Sensors & Actuators: B. Chemical 381 (2023) 133430

Contents lists available at ScienceDirect

Sensors and Actuators: B. Chemical

journal homepage: www.elsevier.com/locate/snb

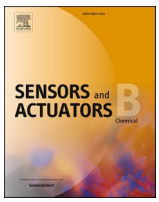

The effects of gas exposure on the graphene/AlGaN/GaN heterostructure under UV irradiation

Katarzyna Drozdowska [a,*], Sergey Rumyantsev [b], Janusz Smulko [a], Andrzej Kwiatkowski [a], Pavlo Sai [b], Paweł Prystawko [c], Aleksandra Krajewska [b], Grzegorz Cywiński [b]

[a] Department of Metrology and Optoelectronics, Faculty of Electronics, Telecommunications, and Informatics, Gdańsk University of Technology, G. Narutowicza 11/12, 80-233 Gdańsk, Poland
[b] CENTERA Laboratories, Institute of High Pressure Physics PAS, Warsaw, Poland
[c] Institute of High Pressure Physics PAS, Warsaw, Poland

ARTICLE INFO

Keywords:
AlGaN-GaN
Graphene
UV-assisted gas sensor
Nitrogen dioxide
Acetone
Tetrahydrofuran

ABSTRACT

This work demonstrates a graphene/AlGaN/GaN sensing device with two-dimensional electron gas (2DEG) toward nitrogen dioxide (NO_2), tetrahydrofuran, and acetone detection under UV light irradiation. We propose combining measurements of the DC characteristics with a fluctuation-enhanced sensing method to provide insight into the gas detection mechanisms in the synergistic structure of highly stable GaN and gas-sensitive graphene. Both DC and low-frequency noise studies reveal the impact of UV irradiation (275 nm) on the GaN-based field-effect transistor (FET). Gas detection improves under UV light with higher differentiability between selected concentrations of inorganic (NO_2) gas and the possibility of discrimination between weakly adsorbing organic species (tetrahydrofuran and acetone). Time-domain experiments confirm the stability and reversibility of sensor (short-time and long-time) responses and reduced time drift after employing UV light. Features observed in the $1/f$ noise spectra may indicate the high impact of the irradiation on the trapping states in the GaN-based heterostructure, which further modulates the fluctuations of the channel carriers in our device. Our findings broaden the view on AlGaN/GaN heterostructures modulated with a graphene gate for gas sensing purposes, including strongly binding inorganic gas and weakly adsorbing organic species.

1. Introduction

Gallium nitride (GaN), a wide bandgap material (~3.4 eV) with high mobility and harsh-environment endurance, offers properties desired for high-power and high-temperature applications and is frequently used in optoelectronics (*e.g.,* LED fabrication) and high-frequency electronics (*e.g.,* RF switches, power devices) [1–4]. Its attractive electronic properties, non-toxicity, and thermal and chemical stability make it also a potential candidate for gas sensing devices. GaN nanoparticles, nanowires, nanotubes, and nanonetworks have been repeatedly demonstrated as gas-sensitive structures over the last decade [5]. GaN nanosheets were studied by first-principle approaches toward small molecule adsorption, revealing the great feasibility of GaN as a highly sensitive sensor [6]. Gas sensors based on GaN were experimentally reported to detect H_2, O_2, NO_2, CO, CH_4, and H_2S [7]. As chemical sensors, GaN platforms were used to sense polar liquids, including ethanol, and as ion-selective field-effect transistors (ISFETs). Moreover, GaN and aluminum gallium nitride (AlGaN) combinations present attractive transport properties and surface sensitivity toward molecular detection [8]. Their heterostructures incorporated in field-effect transistor (FET) devices exhibit two-dimensional electron gas (2DEG) at the AlGaN/GaN interface due to the strong polarization effect, which can be highly sensitive toward surface processes [9,10].

Lately, the combination of GaN nanostructures or AlGaN/GaN heterostructures with graphene for more effective gas sensing has drawn attention. As already known, graphene possesses numerous qualities desired for gas-sensitive materials, such as excellent transport properties, a high surface-to-volume ratio, and a highly active surface of exceptional sensitivity toward molecular processes [11–14]. Hybrids of graphene and GaN-based structures could result in the synergistic effect of combining the high sensitivity observed for graphene-based devices with the chemical, thermal and mechanical stability of GaN. Following this concept, J. Shin et al. proposed a light-assisted NO_2 sensor comprised of graphene and GaN nanowires, in which the GaN operates

* Corresponding author.
E-mail address: katarzyna.drozdowska@pg.edu.pl (K. Drozdowska).

https://doi.org/10.1016/j.snb.2023.133430
Received 4 October 2022; Received in revised form 20 January 2023; Accepted 24 January 2023
Available online 26 January 2023

as a light-absorbing medium while the graphene acts as a channel for the transport of charge carriers [15]. The authors confirmed that only the combination of both materials was selectively responsive toward NO_2, whereas separate graphene or GaN nanowire structures produced inadequate responses. Z. Cui et al. reported first-principles calculations for NO_2, NO, NH_3, and CO adsorption on GaN modified with pristine or defective graphene (g-GaN systems) [16]. Computations for the defective graphene and GaN combination revealed higher adsorption energies, confirming that defects act as additional adsorption centers, leading to higher surface interactions with target molecules. Earlier experimental results also proved higher sensitivity toward gaseous species of defective graphene and are already reviewed in other works [17,18]. Another example of combining an AlGaN/GaN heterojunction with reduced graphene oxide (rGO) can be found in the work of A. Bag et al. [19]. The authors reported a diode gas sensor for NO_2, SO_2, and NH_3 detection, in which the 2D rGO layer is so thin that any surface interactions with gas molecules may not only influence the Fermi level of the rGO but also interact with the extremely sensitive 2DEG at the AlGaN/GaN interface.

Although low-frequency noise measurements of AlGaN/GaN have been conducted for at least a decade, there is still a deficit of noise studies on UV-irradiated structures, especially from the sensing applications point of view. A recent report on AlGaN/GaN high-electron-mobility transistor (HEMT) reveals the dominance of $1/f$ noise in the material that follows the carrier number fluctuations model [20]. In general, the model explains resistance fluctuations in the structure as originating mainly from the carrier concentration fluctuations caused by trapping and de-trapping processes at the surface. For AlGaN/GaN transistors, channel carriers (electrons from 2DEG) can interact with the trap states formed in the AlGaN barrier and GaN bulk layers. It was suggested that $1/f$ noise originates from trapping processes in AlGaN. However, some plateau regions in the spectra may appear due to generation-recombination (GR) centers in the GaN layer for HEMTs with larger channel areas. Another report presents the results of noise studies of UV-enhanced AlGaN/GaN HEMT that also follows the carrier number fluctuation model [21]. In the work, the authors suggest that irradiation with UV light of 365 nm affects trapping states in the GaN buffer leading to the noise originating mainly from the defects in the GaN. The electrical and noise properties of AlGaN/GaN HEMTs with graphene gate were studied by M. Dub et al. [22]. AlGaN/GaN HEMTs with graphene gate demonstrated good current-voltage characteristics and noise of the same order of magnitude as transistors with regular Ni/Au Schottky gate. Moreover, combining DC characteristics with UV light illumination and the fluctuation-enhanced sensing (FES) method for graphene/AlGaN/GaN devices constitutes an intriguing scientific subject.

Herein, we present an AlGaN/GaN FET device with graphene acting as a gate for nitrogen dioxide (NO_2), tetrahydrofuran (C_4H_8O), and acetone (C_3H_6O) sensing, confirming the ability of the structure to detect both inorganic and organic species. Graphene is used for detecting the mentioned vapors [14,23], but other materials and methods are also used for this aim [24–26]. The proposed methods utilize resistance measurements because of their simplicity or optical methods requiring more complicated measurement setups. Graphene or other two-dimensional materials are highly desirable for gas detection because they can reach high sensitivity at simple measurements when detecting volatile organic compounds and some toxic gases emitted by living organisms (*e.g.*, NO_x) [27]. The design of the sensors was initially dedicated to high-frequency applications, and the same device configuration was already reported to act as an RF switch at 70 GHz [28]. We intend to confirm the possibility of utilizing the same hybrid structure of graphene/AlGaN/GaN for UV-enhanced gas sensing implemented with DC characteristics and low-frequency noise measurements. First, we demonstrate the strong influence of UV irradiation on the FET transfer curves regarding various ambient gases. Next, we present gas sensing results in the time domain and confirm the repeatability of the sensor. Lastly, we show the results of low-frequency noise studies and discuss the impact of UV light and different gases on the properties of graphene/AlGaN/GaN FET.

2. Experimental section

2.1. Graphene/AlGaN/GaN sensors fabrication

AlGaN/GaN heterostructures were grown using Metalorganic Vapor Phase Epitaxy (MOVPE) on a commercially available semiisolating silicon carbide (SiC) substrate. The layered AlGaN/GaN heterostructure consisted of an aluminum nitride (AlN) nucleation layer (38 nm) below the GaN buffer of high resistivity (HR GaN, 2.3 μm), and an unintentionally doped GaN layer (UID GaN, 0.7 μm). Next, a top barrier was epitaxially formed consisting of the following layers: 1.2 nm of $Al_xGa_{1-x}N$ ($x = 0.66$); 5 nm of $Al_xGa_{1-x}N$ (UID, $x = 0.28$); 10 nm of AlGaN:Si; and 2 nm of unintentionally doped AlGaN. Finally, the GaN cap covered the heterostructure.

Drain and source electrodes and all metallic pads were thermally evaporated and formed by Ti/Al/Ni/Au of 15 nm/100 nm/40 nm/50 nm thicknesses. Afterward, rapid thermal annealing at 780 °C for 1 min in a nitrogen atmosphere was used for all ohmic contacts to minimize the ohmic contact resistance. After the annealing, the typical value of the contact resistance was ~1 Ω·mm.

The graphene gate was deposited in the last step of the sensors fabrication. We used commercial chemical vapor deposition (CVD) graphene grown on copper foil (Graphenea, San Sebastián, Spain) for our GaN-based sensing device. The high-speed electrochemical delamination technique [29] was employed to transfer PMMA-coated graphene onto the AlGaN/GaN structure. Afterward, the sample was heated at 130 °C for 24 h and then rinsed in acetone to remove the PMMA layer. Finally, the graphene layer was selectively patterned employing laser lithography and etched by reactive ion etching in an oxygen plasma. The patterning made it possible to deposit the graphene between the source and drain contacts with extensions to the side gate pads. The dimensions of the graphene were 10 μm by 60 μm, providing an effective sensing area of 600 μm^2. More details on the properties of the graphene (deposited according to the same procedure), including characterization with Raman spectroscopy, can be found elsewhere [28].

2.2. DC characteristics and noise measurements

DC characteristics and low-frequency noise measurements were performed in a probe station using titanium needles to connect the graphene/AlGaN/GaN sensor's electrodes with the measuring and biasing units. A Keithley-4200A-SCS parameter analyzer with two medium power source-measure units (type 4201-SMU) was used for the transfer curve measurements and time-domain studies. All drain-source current *vs* gate voltage curves (I_{DS} *vs* V_G) were collected in the V_G range from − 5–0 V with a 2 s hold time, and the drain-source voltage (V_{DS}) bias was set to 0.1 V. Time-domain studies were performed at $V_G = -3$ V for dark conditions, and $V_G = -4$ V for the UV-irradiated sensor with V_{DS} set to 0.1 V in both cases.

The sensor was connected to a low-noise preamplifier and current source for noise measurements. The input current was set to 0.553 mA, which resulted in voltage across the sensor V_{DS} of 0.6–0.8 V depending on ambient conditions. Input current I_{DS} between 0.241 mA and 1.140 mA made it possible to measure the $1/f$ noise originating solely from the material without interferences from the system's inherent noise. At the same time, lower I_{DS} currents limited the local heating of the sensor, so the moderate current value of 0.553 mA was chosen for all noise studies. V_G was set to − 3 V and − 4 V for dark and UV-enhanced conditions, respectively, during the noise measurements to correspond to the parameters used in the time-domain studies of I_{DS}. We measured the power spectral density of the voltage fluctuations across the sensor biased by the I_{DS} current utilizing a data acquisition board (National Instruments, model NI USB-4431) and a custom-written LabVIEW program (National

Instruments). We kept the sensor inside a metal shielding box (stainless steel and cobalt foil) to limit external electromagnetic interference during all measurements. The UV-enhanced experiments were performed with a UV LED of maximum optical power at 275 nm (ProLight Opto, type PB2D–1CLA-TC). UV LED was positioned about 1 cm from the sensor's surface, yielding an optical power density of 1.1–1.6 mW/cm^2.

2.3. Gas-sensing experiments

Before the gas sensing experiments, we performed the cleaning procedure by slow heating (at a speed of ~2 °C/min) and annealing the sensor at ~300 °C for 30 min under vacuum conditions (pressure between 1 $\times 10^{-7}$–1.5 $\times 10^{-7}$ mbar). Next, the sensor was left in the vacuum chamber until it naturally cooled down to room temperature. It is worth noting that the cleaning procedure was employed only once, and the device did not require additional refreshing between the gas sensing experiments, offering a high responsivity despite its storage in laboratory air conditions between consecutive sets of studies within at least two weeks of the measurements. The cleaned sample was put into the metal chamber, which provided electromagnetic shielding. The selected gases were transported to the chamber by a metal pipe placed within 0.5 cm from the sample and connected to the gas distribution system. The sensor's response toward nitrogen dioxide, tetrahydrofuran, and acetone was measured. Our primary goal in selecting the ambient atmosphere was to use reducing and oxidizing gases to show the sensor response for two main types of gases. We used the calibration gas of oxidizing NO_2 diluted in nitrogen (N_2) as the carrier gas. To obtain different concentrations of NO_2, we mixed it with pure N_2 at specific proportions while keeping a constant overall gas flow of 50 mL/min. Our laboratory possibilities limited the applied concentrations. With the available gas distribution system, concentrations up to 0.2 ppm of NO_2 could be obtained, but the lowest concentrations needed to be more accurate because of gas flow meter accuracy. For reducing gases, organic vapors were produced by transferring 50 mL/min of N_2 through a glass bubbler with either tetrahydrofuran or acetone solution. In this case, the concentration of the produced organic vapors strictly depends on the dynamic N_2 flow and vapor pressure of the solvent. The estimated concentrations for tetrahydrofuran and acetone were ~100 ppm and ~110 ppm, respectively. The constant overall gas flow was regulated by mass flow controllers (Analyt-MTC, model GFC17). Measurements at varied relative humidity required adjusting the flow of synthetic air through a container with water in 50–200 mL/min range. The DC characteristics and noise spectra were collected after the sensor was subjected to the selected gas for 20 min in dark or UV-enhanced conditions. Before introducing the target gases, UV irradiation was set for ~20 min in a reference atmosphere (laboratory air or N_2). The time-domain curves were checked by introducing the target gas for 10 min and then another 10 min of sensor recovery in N_2 for five repetitions. All experiments were conducted at room temperature (RT ~23 °C) and ambient pressure (~1 bar).

3. Results and discussion

The graphene/AlGaN/GaN used in our sensing experiments works as a FET with graphene exposed to the surrounding atmosphere acting as the third electrode, enabling gate voltage tuning as depicted in Fig. 1. Fig. 1a illustrates a cross-section of the investigated sensor with graphene of an area reaching 600 μm^2. Fig. 1b and c represent optical images in which the small area of graphene is presented with a red dashed contour. The principle of operation of our sensor relies on the surface reactions on the graphene layer, which also modulates the two-dimensional electron gas (2DEG) layer at the AlGaN/GaN interface. In such device configuration, the properties of the graphene are changed with the bias voltage applied between the gate, and the 2DEG channel, so the bias can modulate both layers. Such interesting dependencies between layers in the whole sensor structure could result in unique responses toward different gases present in the ambiance.

Since UV irradiation was previously proved to improve the performance of graphene-based sensors [30,31], we applied a UV LED (275 nm) at selected polarization currents (I_P) to see how it affects the I_{DS}–V_G curves of a graphene/AlGaN/GaN sensor. Both the GaN buffer and AlGaN barrier layer should effectively absorb UV light of the selected wavelength, as its quantum energy exceeds the band gap of these materials. Additionally, we previously confirmed that CVD-grown *p*-doped graphene noticeably responds to UV light (275 nm), so a high irradiation effect on the FET properties is expected [32]. Fig. 2 demonstrates the DC characteristics collected in laboratory air for the device irradiated with a UV LED polarization current I_P between 3 mA and 100 mA. The maximum I_P corresponds to the LED working at its optimal parameters (100% radiant flux). First, one can notice that the threshold voltage (V_{th}) shifts significantly toward negative V_G values for the irradiated sensor. Second, we observe much higher currents in the transistor OFF state under irradiation. Fig. S1 in the supplementary

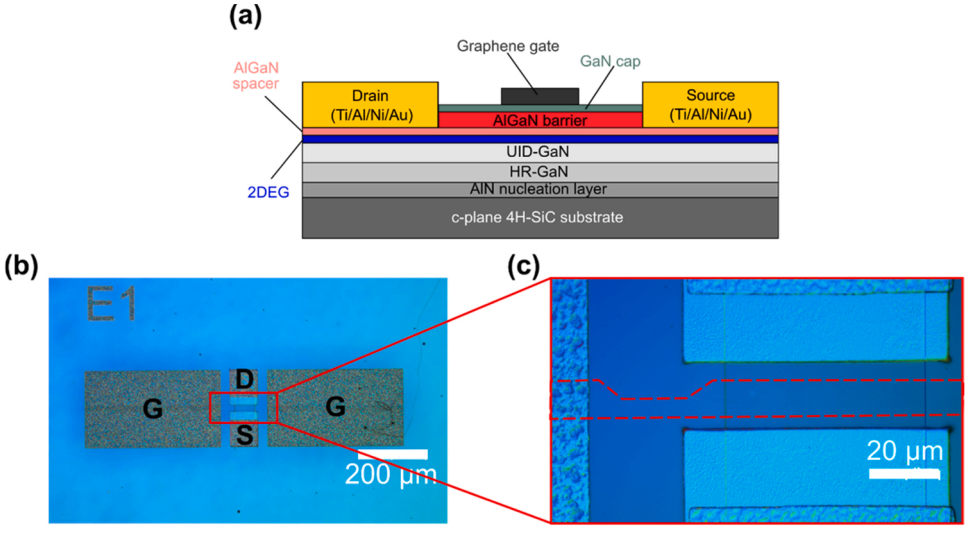

Fig. 1. (a) Schematic representation of investigated structure consisting of AlGaN/GaN layers with graphene gate, (b) real optical image of the exemplary sensor with (c) higher magnification of the graphene monolayer region. Red dashed contour indicates graphene layer (length = 60 μm, width = 10 μm) placement between the source (S) and drain (D) contacts and connection to the gate pads (G).

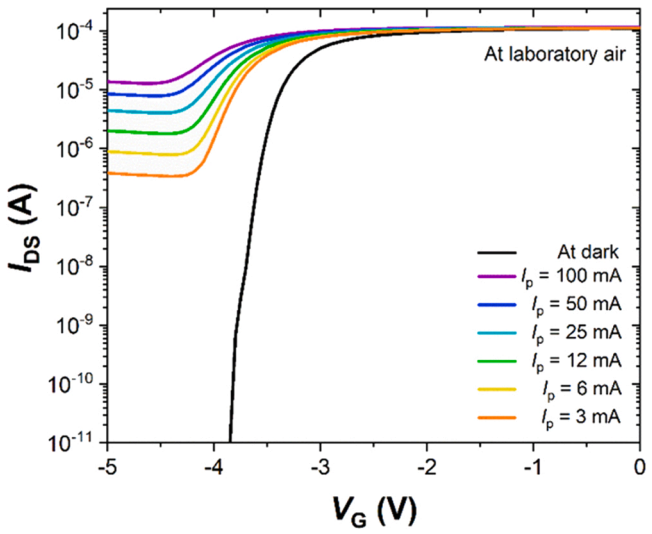

Fig. 2. Drain-source current I_{DS} as a function of gate voltage V_G under laboratory air conditions and for UV LED (275 nm) polarization currents (I_P) between 3 mA and 100 mA.

material depicts the change of V_{th} estimated from the linear extrapolation of the I_{DS}–V_G characteristics. For instance, the threshold voltage was estimated as − 3.45 V in the dark and − 4.39 V for I_P = 100 mA. Generally, the stronger the irradiation and the absorption by the sensing layers, the more significant is the shift. An ON/OFF ratio of around six orders of magnitude was observed previously for these devices under dark conditions and is confirmed by our results [28]. At the same time, the ON/OFF ratio is significantly reduced with UV LED polarized with higher currents. UV light promotes free charge carrier generation, resulting in photocurrent induced in the FET channel. It increases the overall I_{DS} level, which is distinctly visible for V_G values below − 4 V. As mentioned above, the UV light wavelength used in our experiments (275 nm) carries sufficient energy (~4.51 eV) to be absorbed by both the GaN buffer layer and AlGaN barrier layer, so the generation of electron-hole pairs may proceed in both of those regions. The photo-generated electrons increase the charge concentration in 2DEG, thus increasing the drain current and absolute value of the threshold voltage. An additional shift of the threshold voltage may result from the photo-induced holes accumulation in the GaN buffer, as V. Nagarajan et al. described for AlGaN/GaN HEMTs [21]. While the low ON/OFF ratio may constitute a shortcoming in some applications, we opted for choosing the highest UV LED polarization current (100 mA) for all further sensing measurements, as it shifts the DC characteristic most significantly. Thus, the most visible changes may be expected during gas detection. Additionally, we compared sensor I_{DS}-V_G characteristics for laboratory air and inert ambiance of nitrogen to test the influence of humidity present in the open air conditions. Fig. 3a confirms that the impact of humidity is negligible and does not affect sensor transfer characteristic, which is of great benefit for using such sensors in real-environment conditions.

We started the sensing experiments with NO_2, one of the gases that is extremely harmful to humans and the environment, even at relatively low concentrations. Hence, its detection becomes crucial from a practical point of view. Moreover, it is one of the main representatives of the inorganic species for gas detection, characterized by relatively high adsorption energies on different materials. For instance, the adsorption energy of ~1 eV was calculated between NO_2 and a GaN nanotube [33]. Moreover, the adsorption energy and charge transfer indicated the physisorption of NO_2 molecules on the GaN surface. For graphene, computational methods showed that small molecules exhibit physisorption with relatively low adsorption energies [34]. However, the highest values were obtained for NO_2 compared to H_2O, NH_3, CO, and NO. Fig. 4 presents the results of introducing NO_2 at selected concentrations (5–20 ppm) to the sensor, performed in the dark and during UV irradiation. The concentration of 0 ppm presented by the black curves refers to the pure N_2 atmosphere considered a reference in our studies. N_2 was used as a carrier gas in all experiments, but we compared it to the sensor response in the synthetic air (dry synthetic air: pure oxygen 20% and pure nitrogen 80%), which was highly similar to that obtained for the inert ambiance and did not influence FET threshold voltage or saturation point (Fig. 3b). The insets in Fig. 4a confirm that the changes in I_{DS} are more pronounced for the UV-enhanced sensor and gradually shift toward zero V_G for higher NO_2 concentrations. Fig. 4b depicts the negative linear dependence between I_{DS} and the target gas concentration. The results in Fig. 4b show that the device's sensitivity can be optimized by using light-enhanced conditions and adjusting gate voltage bias. Thus, for V_G = −4 V, a lower DL of 2.47 ppm is observed than for V_G = −4.25 V (3.42 ppm) for detection under UV irradiation. Since greater relative changes of drain-source current are observed for the UV-irradiated sensor, the structure is considered to exhibit higher gas sensitivity under light enhancement with lower detection limits (DL). The lower DL was observed at NO_2 concentrations between 0.2 and 2 ppm (Fig. S4 in supplementary materials). Still, the results exhibited limited repeatability due to long-time sensor response (drift) and accuracy of the gas distribution system. The changes of I_{DS} *versus* NO_2 gas

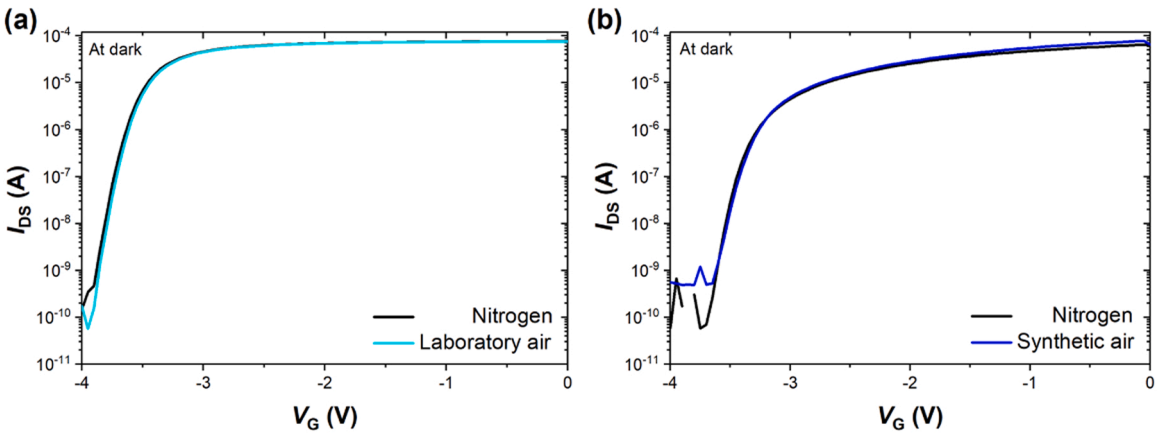

Fig. 3. Comparison of drain-source current I_{DS} as a function of gate voltage V_G applied to the graphene in the dark for nitrogen and (a) laboratory air or (b) synthetic air yielding highly similar characteristics. The level of relative humidity varied between 30% and 50% for the regular indoor environment conditions. As the I_{DS}-V_G curves in (a) and (b) were collected on consecutive days, the minor difference between curves' shape is observed due to the difference in contact between the Ti needles and sensor's electrodes.

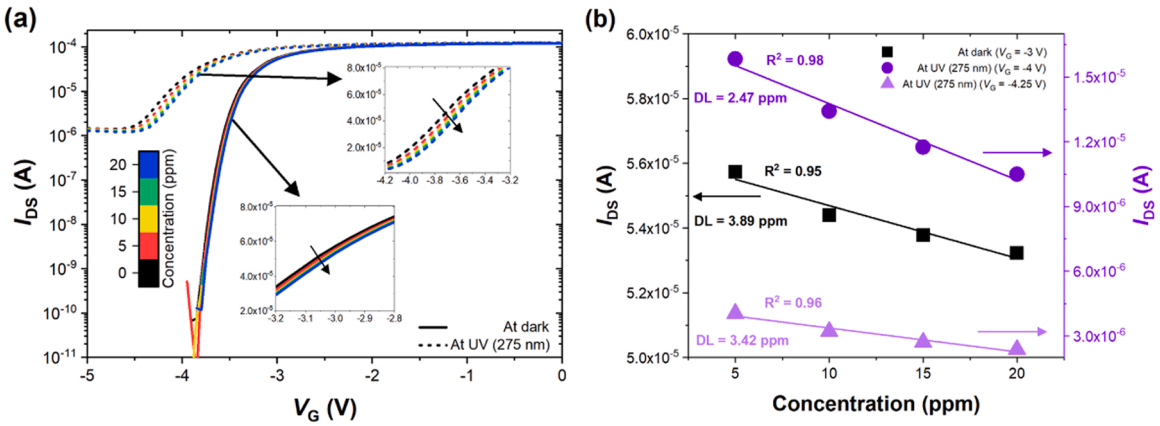

Fig. 4. (a) Drain-source current I_{DS} as a function of gate voltage V_G for different concentrations of NO_2 in the dark (solid curves) and under UV (275 nm) irradiation (dashed curves), and (b) drain-source current I_{DS} as a function of NO_2 concentration in the dark and under UV (275 nm) irradiation showing the linearity of the response. V_G was − 3 V for the dark and − 4 V or − 4.25 V for the irradiated sensor.

concentration (Fig. 4b) consider the response observed during the first cycle of switching on NO_2 flow. It includes two components: the fast response of the sensor to NO_2 taking place within tens of seconds, and partially the long-term drift response taking about 3–4 h in total (Fig. 5). Both components, considered in Fig. 4b, are of similar intensities of a few percent only. We observed that the sensor responded reproducibly on the next experimental day after staying in laboratory air during the night, sufficient to secure its full recovery. Similar observations were presented in the work of A. Bag et al. for a diode sensor based on a rGO and AlGaN/GaN structure [19]. The authors demonstrated that the sensor response *vs* NO_2 concentration follows the Langmuir isotherm equation, which can be simplified to the linear dependence for the low-concentration range. Their findings confirm that the sensitivity decreases with the concentration growth since the surface saturates with gas species, so the response also becomes saturated. Since the response of the graphene/AlGaN/GaN sensor is linear in the selected NO_2 concentration range, we suppose that the saturation level is higher than 20 ppm in the case of our sensor.

Charge transfer is one of the possible interactions that govern the detection process for graphene-based sensors. NO_2 is regarded as a strong oxidizing species that decreases the resistance of *p*-type semiconductors. The CVD-grown graphene used as a gate in our device is characterized by *p*-type conductivity, so the adsorption of oxidizing molecules should increase the concentration of major carriers (holes) in the electrode layer. This effect can be amplified under UV light, presumably owing to the extra electron-hole pairs generated during irradiation and more free charge carriers participating in the surface processes. This way, the ambiance can also influence the gate voltage bias. An alternative explanation is that oxidizing NO_2 creates negatively charged centers in graphene during adsorption, which causes a shift in the threshold voltage. Moreover, our results show that UV light enhances this effect. Additional irradiation may create even more adsorption centers for NO_2 by generating electron-hole pairs in the structure. Photo-induced holes are most probably immediately captured, whereas electrons may remain in the channel. Centers that capture holes become positively charged, facilitating NO_2 adsorption. Our results on NO_2 detection show a subtle shift in the threshold voltage of the AlGaN/GaN transistor toward positive gate voltages for higher gas concentrations. N. Harada et al. demonstrated that the exposure of the graphene gate to gas molecules causes a change in the graphene work function and, consequently, shifts the threshold voltage of silicon transistors [35]. Authors suggest that graphene gate modification by different ambiances can be used for gas sensing purposes, but intentional doping can also tune the FET properties, providing a twofold effect. In the case of the graphene/AlGaN/GaN sensor, we confirm that GaN-based transistor properties can be modified in a similar manner.

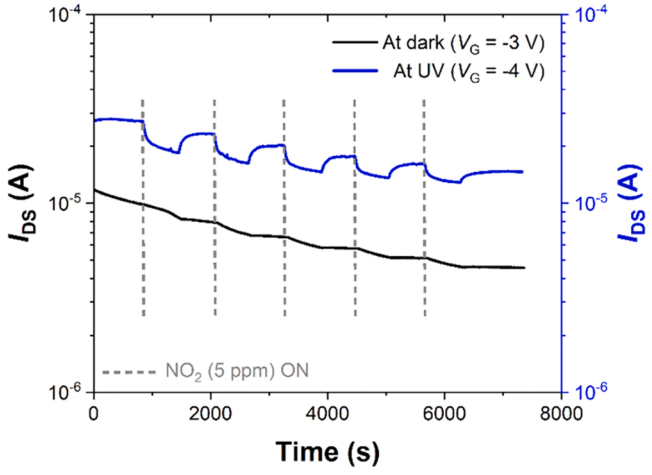

Fig. 5. Drain-source current I_{DS} in the time domain for five repeated cycles of introducing NO_2 (5 ppm). The gate voltage was set to − 3 V and − 4 V for dark and UV-enhanced conditions. Dashed lines indicate the moment when the target gas was introduced to the sensor.

Fig. 5 depicts I_{DS} changes in the time domain for five repetitive cycles of introducing 5 ppm of NO_2 in the dark and under UV irradiation. As can be seen, the graphene/AlGaN/GaN sensor exhibits short-time current drift during the measurements, mostly visible for the first cycle of gas detection. However, UV irradiation contributes to a more pronounced and stable response in each cycle. Again, we see that the sensor response (represented by drain-source current changes) decreases for the detection of 5 ppm of NO_2, which means the overall sensor resistance increases. Since the graphene layer acts as a gate and not a channel, as in most reported graphene-based FET sensors [32,36–38], the ultimate effect of the NO_2 gas is expected to be different in our device. Indeed, for graphene-based sensors characterized by *p*-type conductivity, NO_2 molecules tend to increase the concentration of holes, leading to a resistance decrease [39,40]. In the case of our graphene/AlGaN/GaN device, the opposite result suggests that the change of the fixed charge after gas adsorption on the structure may modulate 2DEG leading to lower channel conductivity and a decrease in I_{DS}. Additionally, the adsorption of molecules can occur at the GaN surface, resulting in a more complex detection mechanism.

As organic molecules are usually more challenging to detect due to their low adsorption energies, we chose tetrahydrofuran and acetone as two common solvents for gas sensing. We produced organic vapors according to the description provided in Experimental Section, with

concentrations relying on the constant carrier gas flow. Fig. 6 presents the I_{DS}–V_G curves for tetrahydrofuran and acetone in the dark and under UV light. Again, we notice a much higher effect of the gas when the sensor is exposed to gases during UV irradiation. Even though both organic vapors are comprised of the same elements (C, H, O), they differ in their structural configuration and basic properties such as polarity and electrical permittivity (exact values can be found in Table S1 for comparison). Thus, their chemical nature could explain the minor differences in their affinity for the graphene gate or GaN layers and the overall influence on the sensor properties.

Similarly to NO_2, we performed time-domain studies for five cycles of tetrahydrofuran (Fig. 7a) or acetone (Fig. 7b) introduction. Once again, we observed highly repetitive and stable responses for UV light enhancement. The summary of the graphene/AlGaN/GaN sensor responses (defined as relative changes of I_{DS} in each detection cycle) can be found in Fig. S2. Our results suggest that UV light accelerates the adsorption and desorption processes and promotes reaching surface equilibrium and stability faster. Moreover, UV irradiation increases the I_{DS} current, which is easier to measure. The simultaneous adsorption and partial desorption occurring at the active surface are supposed to reach equilibrium faster for weakly binding species, thus producing immediate responses. At the same time, the UV light reduces the time drift and improves the desorption since the sensor recovers to its baseline completely after 10 min in N_2 for each cycle. The more negligible drift and faster recovery than in the case of NO_2 can be explained by the presumably higher adsorption energy of NO_2 than tetrahydrofuran or acetone and, thus, weaker desorption. Theoretical studies of the interaction of NO_2 with the graphene surface showed the high importance of defects during adsorption. On the one hand, it may significantly affect sensor sensitivities, but on the other hand, it may require additional force or time for the recovery process [41]. If NO_2 molecules bind strongly to the sensor surface, their incomplete desorption in each cycle gradually shifts the FET sensor properties, resulting in the constant drift visible in the time-domain studies.

The gas-sensing mechanisms can be explained by comparing the presented experimental results with the characteristics observed for the graphene back-gated FET, when the graphene-made channel was situated above the Si/SiO_2 layer [42]. We observed an intense response to tetrahydrofuran gas under UV light for such a sensor. Fourier transform infrared (FTIR) spectra measurements revealed two adsorption bands signaling charge redistribution in the adsorbed tetrahydrofuran ring structure, resulting in DC characteristic shift for this gas only. We did not observe such a DC characteristic shift in the graphene/AlGaN/GaN structure. We suppose that the energy of the adsorption process is lower than in the graphene back-gated FET placed on the Si/SiO_2 layer and does not induce charge redistribution in the ring of adsorbed molecules [42]. We are conscious that it requires more in-depth studies, but this is a rational explanation for the observed gas-sensing differences between the considered sensors. The same mechanism explains slower sensor aging because of the weaker bonding of water molecules from laboratory air. Different substrates for the graphene layer will result in gas sensing alterations that open up new possibilities for modifying the properties of graphene sensors.

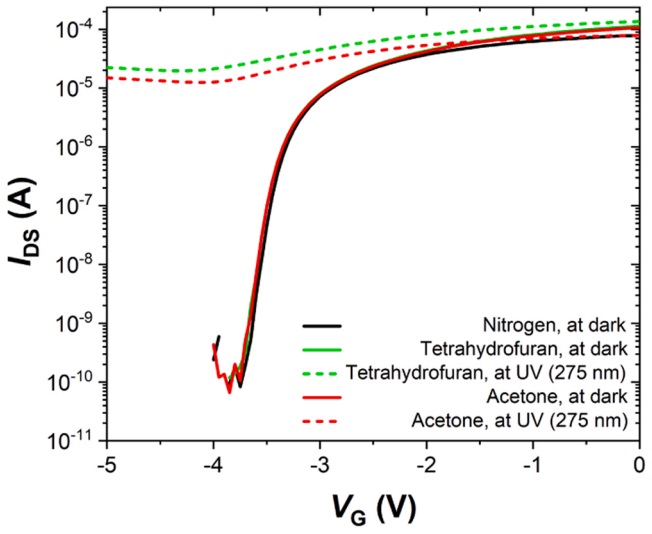

Fig. 6. Drain-source current I_{DS} as a function of gate voltage V_G for tetrahydrofuran and acetone in the dark and under UV (275 nm) irradiation.

Additional experiments with relative humidity variations toward sensor baseline resistance and response to a target gas were conducted to study sensor stability further. Fig. 8 demonstrates relative humidity (RH) variation toward sensor baseline resistance (nitrogen only) and in the presence of acetone (110 ppm) diluted in nitrogen. Interestingly, the baseline remains stable regardless of RH under UV light, but responses to acetone vary for different RH. For dark conditions, the baseline is affected by RH similarly for nitrogen and acetone. Because of severe time drift of sensor response at the ambient atmosphere of NO_2 we could not identify an impact of RH on the measurement results unanimously. Further studies in a more precise gas distribution system are required for NO_2 gas.

Table 1 presents the results of long-term responsivity measurements toward three gases of selected concentrations for dark and UV-enhanced conditions. These measurements were conducted after nine months of the sensor's storage in laboratory air conditions. During this time, the sensor baseline resistance changed from 14.0 kΩ (the value taken from the last measured *I-V* characteristics before more extended storage) to 15.8 kΩ at $V_G = -3$ V (in the dark). Under UV light, the baseline resistance shifted from 2.67 kΩ to 1.66 kΩ at $V_G = -4$ V. The responses for dark conditions remained at the low level of a few %, whereas the responses for UV light conditions were reduced a few times compared to the as-cleaned sensor. The highest resistive response remained for acetone vapor, which was earlier demonstrated to produce the most stable time response (Fig. 7b). The results suggest that long-term stability can be improved by repeating the cleaning procedure to regain sensor performance. However, selected gases still impact sensor *I-V* characteristics after nine months of storage.

Additionally, we propose low-frequency noise studies complementary to DC characteristics measurements for gas sensing purposes. We started with noise measurements for selected concentrations of NO_2 in the dark and under UV irradiation (Fig. 9). Similar to the DC characteristics, we observed comparable noise responses in laboratory air and the inert atmosphere. Therefore, in our discussion, we compare all of the results obtained for target gases to the nitrogen case as a reference. In Fig. 9, we demonstrate $1/f$ noise spectra observed for different concentrations of NO_2, which are modulated mainly by UV light. $1/f$ noise has already been observed in AlGaN/GaN transistors before [20], but the case of UV irradiation was investigated less precisely, especially for gas detection applications. Our results show that sensor irradiation increases the noise level by around one order of magnitude. We see only minor changes in the noise responses for different gas concentrations (mostly for $f \sim 1$ Hz), making it challenging to discriminate between the exact amount of NO_2 traces with only flicker noise measurements either for dark or UV-enhanced conditions.

After completing noise measurements for tetrahydrofuran and acetone, we obtained the same dominating UV light effect as in the case of NO_2 (Fig. 10). Again, we observed a change in the spectrum's shape after irradiation, but in this case, both organic gases decreased the noise level differently. For tetrahydrofuran, the noise level was reduced by ~40% for the lowest frequencies recorded, but the changes were much less visible for acetone. At the same time, we would like to notice highly-repeatable spectra for the reference ambient conditions and the stability of the sensor responses toward both inorganic and organic vapors.

To check the possibility of discrimination amongst various gases, we multiplied the noise spectrum by the frequency for the UV light case, as

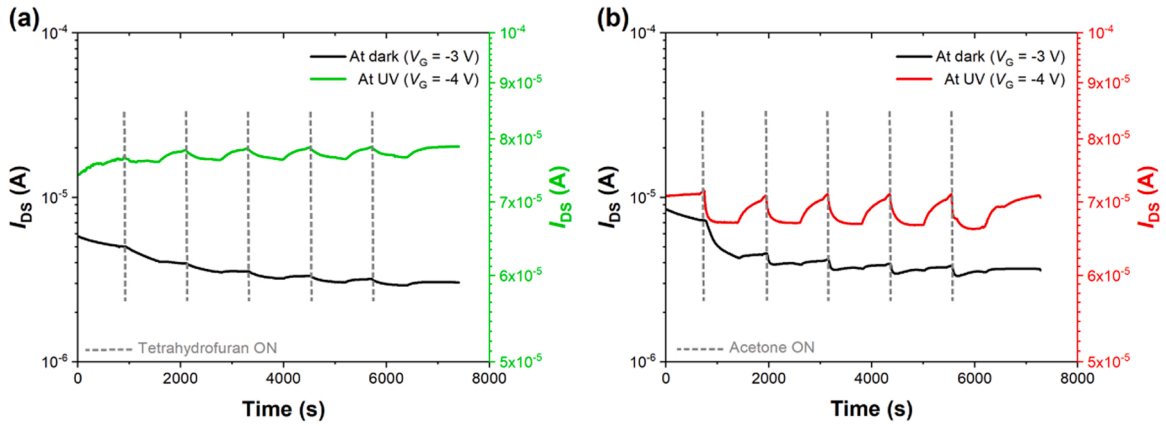

Fig. 7. Drain-source current I_{DS} in the time domain for five repeated cycles of introducing (a) tetrahydrofuran and (b) acetone. The gate voltage was set to − 3 V and − 4 V for dark and UV-enhanced conditions, respectively. Dashed lines indicate the moment when the target gas was introduced to the sensor.

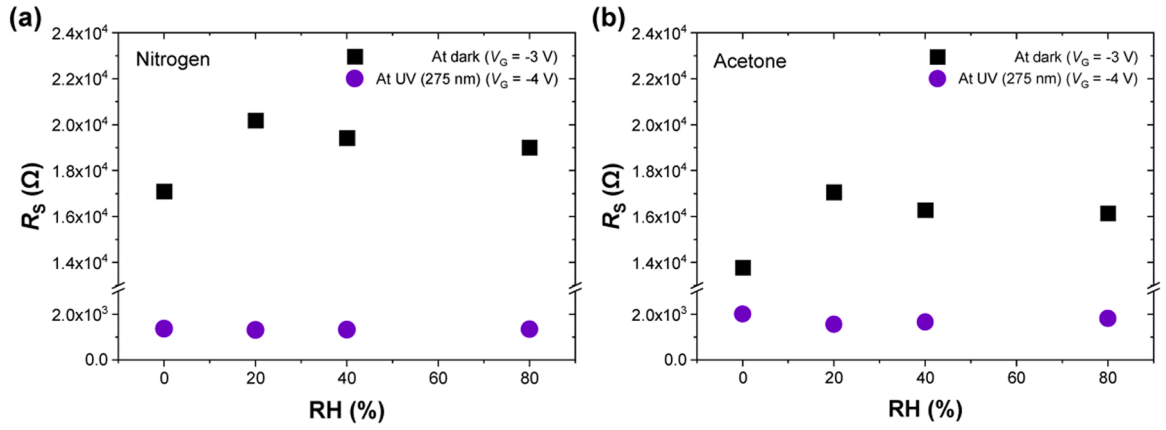

Fig. 8. Changes of sensor resistance R_S *versus* relative humidity (RH) at dark and UV irradiation, and at ambient atmosphere of: (a) nitrogen, (b) acetone diluted in nitrogen (110 ppm).

Table 1
Long-term responsivity of graphene/AlGaN/GaN sensor response toward selected gases. The response was calculated as the absolute value of $(R_S–R_0)/R_0$, where R_S is sensor resistance in the atmosphere of the target gas, and R_0 is sensor baseline resistance (in the reference, nitrogen atmosphere). Resistance values were taken at $V_G = -3$ V for dark and $V_G = -4$ V for UV-enhanced conditions.

Target gas	Response	
	As cleaned (%)	After nine months (%)
Nitrogen dioxide (5 ppm) – dark	2.69	4.69
Nitrogen dioxide (5 ppm) – UV	18.40	2.23
Tetrahydrofuran (100 ppm) – dark	9.08	5.05
Tetrahydrofuran (100 ppm) – UV	8.38	3.27
Acetone (110 ppm) – dark	7.55	3.71
Acetone (110 ppm) – UV	53.60	14.60

illustrated in Fig. 11. We chose only one representative concentration of NO_2 (20 ppm) as highly similar results were obtained for the lower concentrations of the same gas. As can be seen, the spectra vary mainly in the noise level, but the main shape is preserved, confirming the dominating effect of UV irradiation on voltage fluctuations. The local maximum occurs at about 11 Hz, 12 Hz, 13 Hz, and 12 Hz for N_2, acetone, tetrahydrofuran, and 20 ppm of NO_2, respectively, meaning that only minor shifts are introduced with different ambiances. Additionally, Fig. S3 in supplementary materials depicts the reproducibility of the spectra collected for nitrogen during three consecutive days of studies. The local maximum point occurs at ~11 Hz. However, the noise level varies between 1.5×10^{-8}–2.0×10^{-8} for three spectra with a mean value of 1.76×10^{-8} and a standard deviation of 3.19×10^{-9}. Nevertheless, the bulge appearing on all spectra when the sensor is exposed to UV light may imply the influence of irradiation on trapping states in layers surrounding the 2DEG channel, as was previously reported by V. Nagarajan et al. [21]. In the case of our studies, UV light of 275 nm is used for sensor enhancement, so both the GaN and AlGaN layers can absorb it owing to their band gap energies. Therefore, the fluctuations of channel carriers at the interface of the AlGaN/GaN heterostructures can be altered, and deviations from the uniformity of the distribution of the trap states induced by UV light are visible by a local maximum on all UV-enhanced spectra.

4. Conclusions

We demonstrated a graphene/AlGaN/GaN structure for nitrogen dioxide, tetrahydrofuran, and acetone sensing implemented with two complementary methods of DC and low-frequency noise studies. The graphene layer acting as a gate enables gate voltage tuning also by target molecules in the ambiance that can interact with the active layer and affect the electronic properties of graphene. This way, we obtain a change in FET channel conductivity in a few ways. The ultimate result is the synergistic effect of the interaction of both the gate and channel carriers with the ambiance.

UV-enhanced measurements revealed sensor sensitivity to the irradiation itself. Indeed, the GaN layers can effectively absorb UV light of 275 nm, but the irradiation interacts with the graphene surface as well.

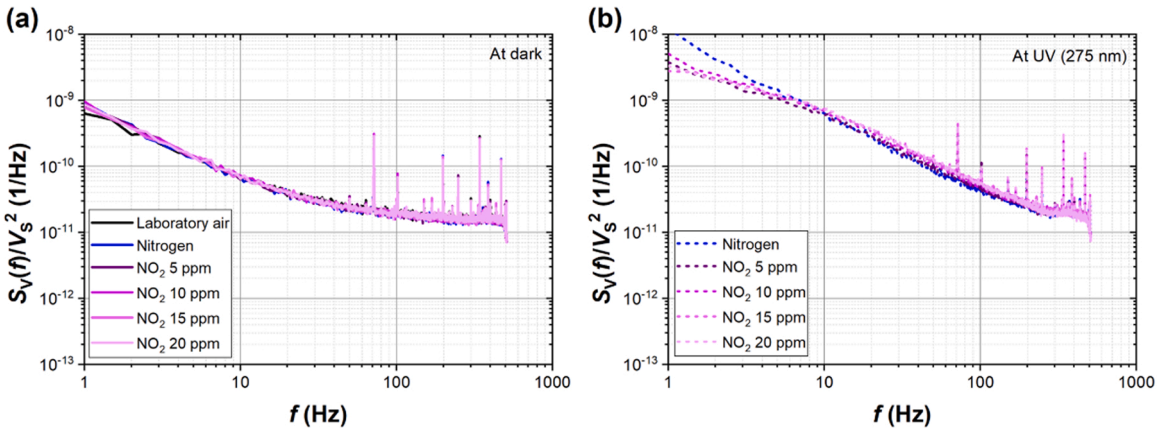

Fig. 9. Power spectral density of voltage fluctuations S_V normalized to sensor DC voltage squared V_S^2 for different concentrations of NO_2 **(a)** in the dark and **(b)** under UV (275 nm) irradiation.

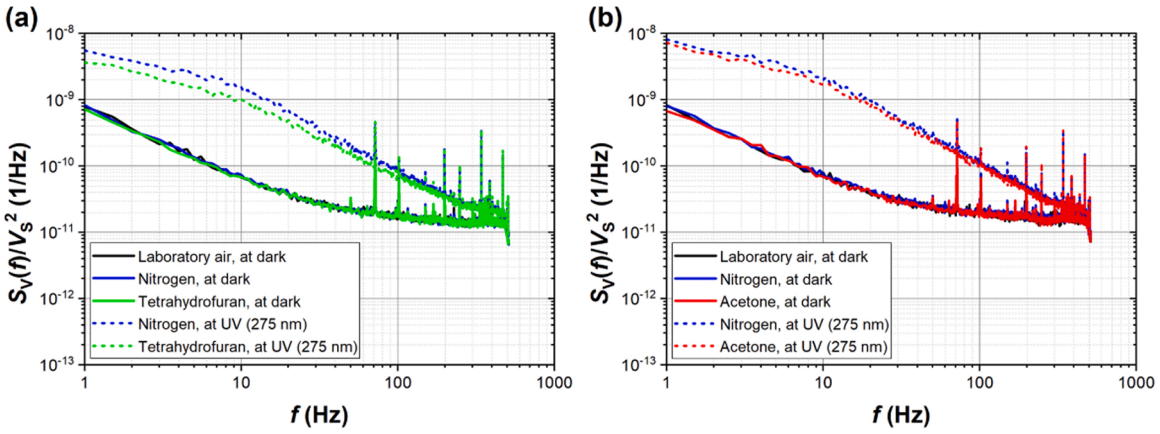

Fig. 10. Power spectral density of voltage fluctuations $S_V(f)$ normalized to sensor DC voltage squared V_S^2 for (a) tetrahydrofuran and (b) acetone in the dark (solid curve) and under 275 nm UV irradiation (dashed curve).

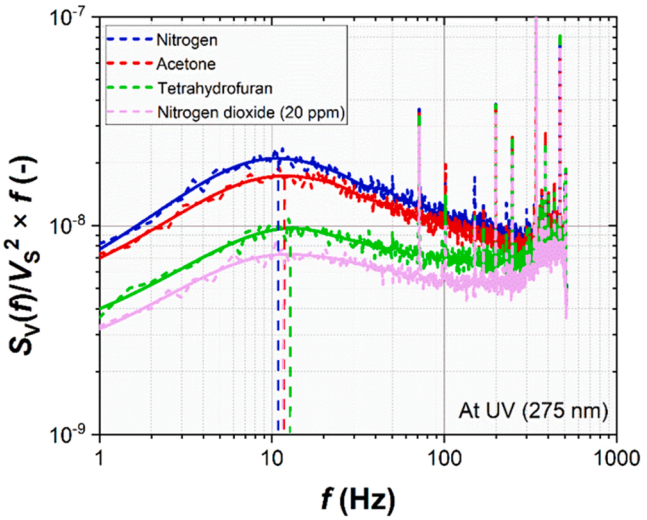

Fig. 11. Comparison of multiplication product of power spectral density of voltage fluctuations $S_V(f)$ normalized to sensor DC voltage squared V_S^2 and frequency f for different vapors. Dashed curves demonstrate experimental data, and solid lines indicate polynomial fitted curves. Vertical dashed lines mark the maximum noise values for fitted functions. Characteristic frequencies occur at about 11 Hz, 12 Hz, 13 Hz, and 12 Hz for nitrogen, acetone, tetrahydrofuran, and 20 ppm of nitrogen dioxide, respectively.

This effect can be an improving factor for accelerated and more stable sensor responses. Additionally, highly similar characteristics obtained for inert ambiance, dry synthetic air, and humid laboratory air indicate the possibility of utilizing graphene/AlGaN/GaN sensor in real-environment conditions, confirmed additionally by study of selected variations of RH toward sensor baseline and response to acetone. For NO_2, discrimination between different concentrations is possible under UV light with DC characteristics, as the responses are linear within the selected concentration range. For organic vapors, UV light improves the selectivity between two solvents (tetrahydrofuran and acetone), making even low responses possible to detect and repeatable. The differences in sensitivity toward the three investigated gases may stem from their various physicochemical properties, such as much higher adsorption energies of inorganic species or differences in structural configurations and polarities between organic vapors. However, we want to note that other characterization methods could be applied to better understand the possible gas sensing mechanisms.

In the case of low-frequency noise measurements, we observed the high impact of UV light on the $1/f$ noise spectra. We assume that the generation of free charge carriers near the 2DEG channel and the influence on the trap states in the AlGaN/GaN absorbing layers may trigger specific fluctuations resulting in a visible bulge at 11–13 Hz. Although we showed that different ambient conditions have a minor effect on the flicker noise, in combination with DC measurements, it not only supports the sensing operation but also sheds light on the possible processes that govern and dominate the detection of gas molecules by the hybrid structure of the graphene/AlGaN/GaN sensor. Overall, we

believe that UV-enhanced graphene/AlGaN/GaN FET sensors shed light on promising effects of UV irradiation for gas-sensing and can result in a new way of developing better gas sensors. A thorough review of carbon-based gas sensors reported elsewhere confirms that their detection begins from about 0.1 ppm of NO_2 [43]. The repeatable detection limit of NO_2 in the studied sensor reached about 2.5 ppm. We observed even one order lower detection limit for this sensor, but its repeatability was much lower. These results suggest that the investigated structure is a strong candidate for NO_2 gas sensor compared to the other reported carbon-based systems.

CRediT authorship contribution statement

S.R. and J.S. conceived the study. K.D. established and ran the experimental studies, evaluated analysis, proposed interpretation, and wrote the text. P.S., P.P., A.Kr., and S.R. fabricated and characterized the samples. S.R., J.S., and G.C. participated in text amendments. A.Kw. participated in laboratory measurements and setup arrangements.

Declaration of Competing Interest

The authors declare that they have no known competing financial interests or personal relationships that could have appeared to influence the work reported in this paper.

Data Availability

Data will be made available on request.

Acknowledgments

This work was funded by the National Science Centre, Poland, the research project: 2019/35/B/ST7/02370 “System of gas detection by two-dimensional materials”. This work was also partially supported by the “International Research Agendas” program of the Foundation for Polish Science co-financed by the European Union under the European Regional Development Fund (No. MAB/2018/9). A. Krajewska was supported by the Foundation for Polish Science (FNP).

Appendix A. Supporting information

Supplementary data associated with this article can be found in the online version at doi:10.1016/j.snb.2023.133430.

References

[1] R. Sokolovskij, J. Zhang, Y. Jiang, G. Chen, G.Q. Zhang, H. Yu, AlGaN/GaN HEMT micro-sensor technology for gas sensing applications, 2018 14th IEEE Int. Conf. Solid-State Integr. Circuit Technol. ICSICT 2018 - Proc. (2018) 2–5. https://doi.org/10.1109/ICSICT.2018.8564904.
[2] M.S. Kang, C.H. Lee, J.B. Park, H. Yoo, G.C. Yi, Gallium nitride nanostructures for light-emitting diode applications, Nano Energy 1 (2012) 391–400, https://doi.org/10.1016/J.NANOEN.2012.03.005.
[3] N.R. Glavin, K.D. Chabak, E.R. Heller, E.A. Moore, T.A. Prusnick, B. Maruyama, D. E. Walker Jr, D.L. Dorsey, Q. Paduano, M.N. Snure, R. Glavin, E.R. Heller, E. A. Moore, B. Maruyama, D.L. Dorsey, K.D. Chabak, T.A. Prusnick, D.E. Walker Jr, Q. Paduano, M. Snure, Flexible gallium nitride for high-performance, strainable radio-frequency devices, Adv. Mater. 29 (2017) 1701838, https://doi.org/10.1002/ADMA.201701838.
[4] S. Mudassir, J. Muhammad, A review of gallium nitride (GaN) based devices for high power and high frequency applications, J. Appl. Emerg. Sc. 4 (2013).
[5] M.A.H. Khan, M.V. Rao, Gallium Nitride (GaN) nanostructures and their gas sensing properties: a review, Sensors 20 (2020).
[6] Y. Yong, H. Cui, Q. Zhou, X. Su, Y. Kuang, X. Li, Adsorption of gas molecules on a graphitic GaN sheet and its implications for molecule sensors, RSC Adv. 7 (2017) 51027–51035, https://doi.org/10.1039/c7ra11106a.
[7] K.T. Upadhyay, M.K. Chattopadhyay, Sensor applications based on AlGaN/GaN heterostructures, Mater. Sci. Eng. B Solid-State Mater. Adv. Technol. 263 (2021), 114849, https://doi.org/10.1016/j.mseb.2020.114849.
[8] A. Ranjan, M. Agrawal, K. Radhakrishnan, N. Dharmarasu, AlGaN / GaN HEMT-based high-sensitive NO 2 gas sensors, Jpn. J. Appl. Phys. 58 (2019) 1–6.
[9] S.A. Eliza, A.K. Dutta, Ultra-high sensitivity gas sensors based on GaN HEMT structures, ICECE 2010 - 6th Int. Conf. Electr. Comput. Eng. (2010) 431–433. ⟨https://doi.org/10.1109/ICELCE.2010.5700721⟩.
[10] J. Sun, R. Sokolovskij, E. Iervolino, Z. Liu, P.M. Sarro, G. Zhang, Suspended AlGaN/GaN HEMT NO2 Gas Sensor Integrated with Micro-heater, J. Micro Syst. 28 (2019) 997–1004, https://doi.org/10.1109/JMEMS.2019.2943403.
[11] A. Nag, A. Mitra, S.C. Mukhopadhyay, Graphene and its sensor-based applications: a review, Sens. Actuators, A Phys. 270 (2018) 177–194, https://doi.org/10.1016/j.sna.2017.12.028.
[12] S.S. Varghese, S. Lonkar, K.K. Singh, S. Swaminathan, A. Abdala, Recent advances in graphene based gas sensors, Sens. Actuators B Chem. 218 (2015) 160–183, https://doi.org/10.1016/j.snb.2015.04.062.
[13] F.L. Meng, Z. Guo, X.J. Huang, Graphene-based hybrids for chemiresistive gas sensors, TrAC - Trends Anal. Chem. 68 (2015) 37–47, https://doi.org/10.1016/j.trac.2015.02.008.
[14] N. Zheng, L. Wang, H. Wang, J. Gao, X. Dong, Y.W. Mai, Conductive graphite nanoplatelets (GNPs)/polyethersulfone (PES) composites with inter-connective porous structure for chemical vapor sensing, Compos. Sci. Technol. 184 (2019), 107883, https://doi.org/10.1016/J.COMPSCITECH.2019.107883.
[15] J. Shin, S. Han, S. Noh, Y.-T. Yu, J.S. Kim, Room-temperature operation of light-assisted NO 2 gas sensor based on GaN nanowires and graphene, Nanotechnology 32 (2021), 505201, https://doi.org/10.1088/1361-6528/ac2427.
[16] Z. Cui, X. Wang, Y. Ding, E. Li, K. Bai, J. Zheng, T. Liu, Adsorption of CO, NH3, NO, and NO2 on pristine and defective g-GaN: improved gas sensing and functionalization, Appl. Surf. Sci. 530 (2020), 147275, https://doi.org/10.1016/j.apsusc.2020.147275.
[17] C. Anichini, W. Czepa, D. Pakulski, A. Aliprandi, A. Ciesielski, P. Samorì, Chemical sensing with 2D materials, Chem. Soc. Rev. 47 (2018) 4860–4908, https://doi.org/10.1039/c8cs00417j.
[18] H. Cruz-martínez, H. Rojas-chávez, F. Montejo-alvaro, Y.A. Peña-castañeda, P. T. Matadamas-ortiz, D.I. Medina, Recent developments in graphene-based toxic gas sensors: a theoretical overview, Sensors 21 (2021) 1–17, https://doi.org/10.3390/s21061992.
[19] A. Bag, D. Bin Moon, K.H. Park, C.Y. Cho, N.E. Lee, Room-temperature-operated fast and reversible vertical-heterostructure-diode gas sensor composed of reduced graphene oxide and AlGaN/GaN, Sens. Actuators B Chem. 296 (2019), 126684, https://doi.org/10.1016/j.snb.2019.126684.
[20] M. Glória Caño de Andrade, L. Felipe de Oliveira Bergamim, B. Baptista Júnior, C. Roberto Nogueira, F. Alex da Silva, K. Takakura, B. Parvais, E. Simoen, Low-Frequency noise investigation of AlGaN/GaN high-electron-mobility transistors, Solid. State Electron. 183 (2021), 108050, https://doi.org/10.1016/J.SSE.2021.108050.
[21] V. Nagarajan, K. Chen, H. Lin, H. Hu, G. Huang, C. Lin, B. Chen, S. Member, D. Anandan, S.K. Singh, C. Wu, E.Y. Chang, Low-Frequency noise characterization of AlGaN / GaN HEMTs and MIS-HEMTs, IEEE Trans. Nanotechnol. 19 (2020) 405–409, https://doi.org/10.1109/TNANO.2020.2992732.
[22] M. Dub, P. Sai, A. Przewłoka, A. Krajewska, M. Sakowicz, P. Prystawko, J. Kacperski, I. Pasternak, G. Cywiński, D. But, W. Knap, S. Rumyantsev, Graphene as a schottky barrier contact to AlGaN/GaN heterostructures, Materials 13 (2020), https://doi.org/10.3390/MA13184140.
[23] S. Some, Y. Xu, Y. Kim, Y. Yoon, H. Qin, A. Kulkarni, T. Kim, H. Lee, Highly sensitive and selective gas sensor using hydrophilic and hydrophobic graphenes, Sci. Rep. 3 (2013) 1–8, https://doi.org/10.1038/srep01868.
[24] A.J. Matzger, C.E. Lawrence, R.H. Grubbs, N.S. Lewis, Combinatorial approaches to the synthesis of vapor detector arrays for use in an electronic nose, J. Comb. Chem. 2 (2000) 301–304, https://doi.org/10.1021/cc990056t.
[25] Z.Y. Xu, L. Han, X.H. Wang, J.R. Chen, N.B. Li, H.Q. Luo, Rational construction of long-wavelength emissive AIE molecules and their application for sensitive and visual detection of HClO, Sens. Actuators B Chem. 352 (2022), 131024, https://doi.org/10.1016/J.SNB.2021.131024.
[26] S. Cui, B. Wang, Y. Teng, Z. Wan, Y. Zan, L. Chen, Y. Li, X. Yan, Highly sensitive sensing of polarity, temperature, and acid gases by a smart fluorescent molecule, Sens. Actuators B Chem. 344 (2021), 130120, https://doi.org/10.1016/J.SNB.2021.130120.
[27] L. Zhang, K. Khan, J. Zou, H. Zhang, Y. Li, Recent advances in emerging 2D material-based gas sensors: potential in disease diagnosis, Adv. Mater. Interfaces 6 (2019) 1–27, https://doi.org/10.1002/admi.201901329.
[28] Y. Yashchyshyn, P. Bajurko, J. Sobolewski, P. Sai, A. Przewłoka, A. Krajewska, P. Prystawko, M. Dub, W. Knap, S. Rumyantsev, Graphene / AlGaN / GaN RF switch, Micromachines 12 (2021) 1–11.
[29] T. Ciuk, I. Pasternak, A. Krajewska, J. Sobieski, P. Caban, J. Szmidt, W. Strupinski, Properties of chemical vapor deposition graphene transferred by high-speed electrochemical delamination, J. Phys. Chem. C. 117 (2013) 20833–20837, https://doi.org/10.1021/JP4032139/ASSET/IMAGES/LARGE/JP-2013-032139_0006.JPEG.
[30] J. Zhang, X. Liu, G. Neri, N. Pinna, Nanostructured materials for room-temperature gas sensors, Adv. Mater. 28 (2016) 795–831, https://doi.org/10.1002/adma.201503825.
[31] R. Kumar, X. Liu, J. Zhang, M. Kumar, Room-Temperature gas sensors under photoactivation: from metal oxides to 2D materials, Nano-Micro Lett. 12 (2020), https://doi.org/10.1007/s40820-020-00503-4.
[32] K. Drozdowska, A. Rehman, P. Sai, B. Stonio, A. Krajewska, G. Cywiński, M. Haras, S. Rumyantsev, J. Smulko, A. Kwiatkowski, Pulsed UV-irradiated graphene sensors for ethanol detection at room temperature, in: Proc. IEEE Sensors, IEEE, 2021, https://doi.org/10.1109/sensors47087.2021.9639514.

[33] M.S. Khan, A. Srivastava, NH3 and NO2 adsorption analysis of GaN nanotube: a first principle investigation, J. Electroanal. Chem. 775 (2016) 243–250, https://doi.org/10.1016/J.JELECHEM.2016.05.048.
[34] O. Leenaerts, B. Partoens, F.M. Peeters, Adsorption of H2O, NH3, CO, NO2, and NO on graphene: a first-principles study, Phys. Rev. B 77 (2008) 1–6, https://doi.org/10.1103/PhysRevB.77.125416.
[35] N. Harada, K. Hayashi, M. Kataoka, J. Yamaguchi, M. Ohtomo, M. Ohfuchi, I. Soga, D. Kondo, T. Iwai, S. Sato, Graphene-gate transistors for gas sensing and threshold control, Tech. Dig. - Int. Electron Devices Meet. Iedm. (2017) 18.2.1–18.2.4, https://doi.org/10.1109/IEDM.2016.7838444.
[36] T. Hayasaka, Y. Kubota, Y. Liu, L. Lin, The influences of temperature, humidity, and O2 on electrical properties of graphene FETs, Sens. Actuators B Chem. 285 (2019) 116–122, https://doi.org/10.1016/j.snb.2019.01.037.
[37] T. Hayasaka, A. Lin, V.C. Copa, L.P. Lopez, R.A. Loberternos, L.I.M. Ballesteros, Y. Kubota, Y. Liu, A.A. Salvador, L. Lin, An electronic nose using a single graphene FET and machine learning for water, methanol, and ethanol, Microsyst. Nanoeng. 6 (2020), https://doi.org/10.1038/s41378-020-0161-3.
[38] P. Bhattacharyya, Fabrication strategies and measurement techniques for performance improvement of graphene/graphene derivative based FET gas sensor devices: a review, IEEE Sens. J. 21 (2021) 10231–10240, https://doi.org/10.1109/JSEN.2021.3060463.
[39] X. Yan, Y. Wu, R. Li, C. Shi, R. Moro, Y. Ma, L. Ma, High-Performance UV-Assisted NO2 sensor based on chemical vapor deposition graphene at room temperature, ACS Omega 4 (2019) 14179–14187, https://doi.org/10.1021/acsomega.9b00935.
[40] C.M. Yang, T.C. Chen, Y.C. Yang, M. Meyyappan, Annealing effect on UV-illuminated recovery in gas response of graphene-based NO2 sensors, RSC Adv. 9 (2019) 23343–23351, https://doi.org/10.1039/c9ra01295h.
[41] Y. You, J. Deng, X. Tan, N. Gorjizadeh, M. Yoshimura, S.C. Smith, V. Sahajwalla, R. K. Joshi, On the mechanism of gas adsorption for pristine, defective and functionalized graphene, Phys. Chem. Chem. Phys. 19 (2017) 6051, https://doi.org/10.1039/c6cp07654h.
[42] K. Drozdowska, A. Rehman, P. Sai, B. Stonio, A. Krajewska, M. Haras, S. Rumyantsev, O. Lars, Organic vapor sensing mechanisms by large-area graphene back- gated field-effect transistors under UV irradiation, ACS Sens. (2022), https://doi.org/10.1021/acssensors.2c01511.
[43] S.W. Lee, W. Lee, Y. Hong, G. Lee, D.S. Yoon, Recent advances in carbon material-based NO2 gas sensors, Sens. Actuators, B Chem. 255 (2018) 1788–1804, https://doi.org/10.1016/J.SNB.2017.08.203.

Katarzyna Drozdowska received her M.Sc. degree in nanotechnology from Gdańsk University of Technology, Poland, in 2020. During her studies, she took a traineeship at Max Planck Institute for Polymer Research, Mainz, Germany (2018), where she investigated thin-film transistors based on organic substances. Currently, she is pursuing her Ph. D. studies at the Department of Metrology and Optoelectronics in the field of electronics. Her main research focus concerns low-dimensional materials for gas sensing devices, utilizing light modulation and 1/f noise for more sensitive and selective detection of volatile compounds.

Sergey Rumyantsev received the M.S.E.E. degree from Leningrad Electrotechnical Institute, Leningrad, USSR, in 1977, the Ph.D. degree in physics from Leningrad Polytechnical Institute in 1986, and the Doctor of Science (Habilitation) degree from A.F. Ioffe Institute in 1996. From 1977–2018, he was with A.F. Ioffe Institute. From 1999 he was also with Rensselaer Polytechnic Institute, USA. In 2018 he joined Institute of High-Pressure Physics, Polish Academy of Sciences. He was a visiting professor of Simon Frazer Univ., Vancouver, Canada, University of Montpellier, Montpellier, France, University of Riverside, California. He published More than 200 papers in refereed journals, presented More than 200 invited, keynote, and contributed talks at International Conferences, and authored, co-authored, or edited 7 books. Area of the expertise includes terahertz electronics, noise in electronic devices and nanostructures (graphene, carbon nanotubes, van der Waals materials), wide band gap semiconductors: SiC, GaN, CdS, 1/f noise for gas sensing.

Janusz Smulko received his M.Sc., Ph.D. and D.Sc. degrees in electronics from Gdańsk University of Technology, Poland, in 1989, 1996 and 2007, respectively. Presently, he is a full professor (since 2016), Head of the Metrology and Optoelectronics Department (since 2012). He had also conducted scientific research in short-term positions at Texas A&M University (2003), Uppsala University (2006/07), Massachusetts Institute of Technology (2011, 2013). As a researcher, he focuses on the applications of 1/f noise for gas sensing and reliability assessment of electronic components and structures, the influence of noise on detection efficiency in Raman spectroscopy systems. He was Vice-Rector for Research of the Gdańsk University of Technology (in the term 2016–2019), member of the Committee on Metrology and Scientific Instrumentation of the Polish Academy of Science (two terms: 2013–2019) and Editor-in-Chief of Metrology and Measurement Systems Journal (two terms: 2013–2019), Chair of IEEE Chapter Computer Society Gdańsk (two terms: 2014–2017). Professor chaired three International Conferences on Noise and Fluctuations issues and managed seven research projects. He was a member of the H2020-MSCA-RISE-2014 project TROPSENSE: "Development of a non-invasive breath test for early diagnosis of tropical diseases" (No: 645758) and co-authored more than 120 papers.

Andrzej Kwiatkowski has graduated from the Gdańsk University of Technology and defended his Ph.D. (Raman spectra processing algorithms in the process of chemical substances detection) at the Faculty of Electronics, Telecommunications, and Informatics in 2014. He published papers about data processing for chemical compounds or gas detection by signal processing methods (pre-processing methods and detection algorithms: SVM, PCA and correlation algorithms). Dr. Kwiatkowski specializes in the design and programming of embedded systems. He was involved in numerous research projects and was responsible for software preparation controlling the dedicated one-board computers (*e.g.* portable Raman spectrometer - 2011, electronic nose - 2019, exhaled breath analyzer - 2021). In 2017 and 2018, he completed a three-month internship at JLM Innovation GmbH (Tübingen, Germany), where he participated in the development of breath sample analysis devices.

Pavlo Sai obtained his M.Sc. degree in Physics from Faculty of Physics and mathematics at Zhytomyr Ivan Franko State University, Ukraine, in 2015. He has three years' experience as engineer in laboratory of physical and technological problems of solid-state microwave electronics at V.E. Lashkaryov Institute of Semiconductor Physics NAS of Ukraine. Currently he is a Ph.D. student in THz laboratory at Institute of High Pressure Physics of the Polish Academy of Sciences. Since 2018, he joined CENTERA Project as an assistant. His main scientific interests are: AlGaN/GaN high electron mobility transistors with Graphene integration; GaN-based plasmonic devices for terahertz spectral range application; grating-based metamaterials for amplification and generation of terahertz radiation.

Pawel Prystawko received the M.Sc.E.E. degree from Faculty of Electronics, Warsaw University of Technology in 1996, the Ph.D. degree in physics from Institute of Physics, Polish Academy of Sciences, Warsaw in 2002. From 1995 he was with High Pressure Research Center Unipress, Warsaw Poland which is now Institute of High Pressure of Polish Academy of Sciences. He is also co-founder of TopGaN Ltd, spin-off company in 2002 from Institute of High Pressure Physics for commercialization of laser diode technologies, from 2002 MOCVD Scientist in TopGaN Ltd. His professional interests are semiconductor physics and technologies of devices based on nitrides. He is experienced in metallorganic vapor phase epitaxy. Scientific interests design of growth MOCVD processes of Nitride structures, point defects in semiconductors, vertical electronic devices (transistors) based on GaN derivatives as well as *in-situ* monitoring of the growth processes. He authored and co-authored more than 135 publications and has H-index of 21.

Aleksandra Krajewska, Ph.D. (female) is a research assistant in CENTERA Labs. She obtained the title of M.Sc. in Chemistry at the Military University of Technology (WAT) in 2012. In 2019 earned Doctor's degree at the same University for the thesis entitled "Modification of graphene structure for photonic and electronic applications". After obtaining M.Sc. degree she enrolled at ITME as an engineer, later to become Engineer Specialist. As a researcher at ITME and Ph.D. student at WAT she was involved in electrical and materials characterization as well as in the development of a method for graphene transfer from metals to arbitrary substrates and chemical modification of graphene properties. In 2019 she moved to the Center for Terahertz Research and Applications CENTERA in Warsaw. Her scientific Author Biographies Click here to view linked References background is closely related to carbon-based materials and 2D materials, *i.e.* graphene, nanotube, MoS2, hBN and their possible applications in electronic systems as well as in other related applications. Her academic achievements include more than 40 scientific articles in the carbon-related area.

Grzegorz Cywiński obtained his Master of Science and Bachelor degrees in the field of microelectronics and semiconductor instruments from the Electrotechnical University, St. Petersburg, Russia in 1995. He received the Ph.D. degree in Physics in Semiconductor Physics from the Institute of Physics of the Polish Academy of Sciences, Warsaw, Poland, in 2004 and then habilitation degree in Physics from the Institute of High Pressure Physics of the Polish Academy of Sciences (IHPP PAS), Warsaw, Poland, in 2020. Since September 2020 he is the Scientific Affairs Director of the CENTERA Labs at IHPP PAS. His professional interests are semiconductor physics and technologies of devices based on tellurides, nitrides and divers 2D materials. He is experienced in molecular beam epitaxy (tellurides, nitrides, and selenides), processing, technology, and applications of devices based on them. Recently, his scientific interests are focused on novel designs and concepts of devices for high frequency research and their applications (including terahertz, subterahertz, and mm-waves ranges). Grzegorz Cywiński is an author or co-author of more than 100 original papers in previewed scientific journals.